J. Fluid Mech. (1997), *vol.* 333, *pp.* 273–299

Scattering of sound waves by a cylindrical vortex: a semi-analytical theory

By J. REINSCHKE†, W. MÖHRING AND F. OBERMEIER

MPI für Strömungsforschung, Bunsenstraße 10, D–37073 Göttingen, Germany

(Received 29 December 1994 and in revised form 1 October 1996)

A semi-analytical theory for the scattering of plane sound waves by a compressible, non-homentropic, circular-cylindrical, single vortex is presented in this paper. As a special case, the scattering of sound by a cylindrical inhomogeneity (hot spot) is investigated. Contrary to the otherwise analogous quantum-mechanical scattering problem, there are singularities in the modified acoustic wave equation for radii $x_s \in (0, \infty)$ when the scattering by a vortex is considered. It will be shown how these singularities can be treated.

This sound-scattering theory is applied to the problem of the interaction of weak plane shock waves with a strong cylindrical vortex. The calculated scattered sound signal has a rather complicated structure in which a cylindrical wave with an essentially quadrupolar directivity pattern is discernible. In the case of shock–hot-spot interaction a scattered sound signal with dipole-like amplitude is obtained. Both results qualitatively agree with experimental findings.

1. Introduction

Knowledge of sound scattering by a vortical flow field is a prerequisite for many aeroacoustic calculations. A prototype of this general problem is the scattering of plane sound waves by a single cylindrical vortex. As a 'direct' problem, its understanding is also the first step towards the solution of the 'inverse' problem, i.e. the determination of vortex location and strength by means of the scattered sound signal, which is of practical importance for aircraft transport (Ferziger 1974).

The problem of scattering of sound waves by a vortex has been considered by numerous authors during the last few decades (e.g. Müller & Matschat 1959; Fetter 1964; Obermeier 1968; O'Shea 1975; Broadbent 1977; Kambe & Mya Oo 1981; Kambe 1982; Howe 1983; Klimow 1988 and Colonius, Lele & Moin 1994). For a brief summary of the crucial assumptions and results of most of the quoted authors we refer the reader to the article by Colonius *et al.* (1994).

With the exception of the numerical calculation carried out by Colonius *et al.* (1994), the different theoretical approaches make the following assumptions: the maximum azimuthal base-flow velocity is small compared to the sound velocity, the base flow is incompressible and homentropic, the theory is only applicable for very specific vortex models, namely potential or Rankine vortices (see §2), and either the acoustic wavelength is regarded small or the vortex is assumed acoustically compact. The present approach developed in §3 tackles the problem without making any of

† Present address: Department of Engineering, University of Cambridge, Trumpington Street, Cambridge CB2 1PZ, UK.

these assumptions. This is necessary since we want to apply the sound-scattering theory to the problem of shock–vortex interaction, considering an experimental set-up where vortices and shocks are produced in the same flow. Such experiments have been carried out by several groups. Mandella & Bershader (1987) investigated the structure of a single compressible cylindrical vortex. Their results will be summed up in §2. The works of Hollingsworth & Richards (1955) as well as Dosanjh & Weeks (1965) focus on shock–vortex interaction. Their experimental findings are compared with our theoretical results in §4. Shock–hot-spot interaction is also considered in this section.

To facilitate the readability, a list of variables and symbols that occur in several places throughout the article is given in Appendix A.

2. Vortex models

Throughout the article we use a cylindrical coordinate system (r, ϕ, z), where the z-axis coincides with the symmetry axis of the vortex. The velocity field of the base flow is given by $\bar{\boldsymbol{v}} = (\bar{u}, \bar{v}, \bar{w})$. One generally assumes that the radial and axial velocity components $\bar{u}$ and $\bar{w}$ are negligible in comparison to the azimuthal component $\bar{v}$. This is confirmed by experiments. In the case of a potential vortex, the velocity vector reduces to $\bar{\boldsymbol{v}} = (0, \bar{\Gamma}_\infty/2\pi r, 0)$, where $\bar{\Gamma}_\infty$ denotes the base flow circulation. For a Rankine vortex,

$$\bar{v}(r) = \begin{cases} \bar{\Gamma}_\infty r/(2\,\pi\,R^2) & \text{for} \quad r < R, \\ \bar{\Gamma}_\infty/(2\,\pi\,r) & \text{for} \quad r > R. \end{cases} \tag{2.1}$$

The radius $r = R$, where the azimuthal velocity assumes its maximum value, is called the *vortex radius*. For an incompressible vortex, the azimuthal velocity is governed by the azimuthal Navier–Stokes equation

$$\frac{\partial \bar{v}(r,t)}{\partial t} = \bar{\nu}\left(\frac{\partial^2 \bar{v}}{\partial r^2} + \frac{1}{r}\frac{\partial \bar{v}}{\partial r} - \frac{\bar{v}}{r^2}\right). \tag{2.2}$$

The variable $\bar{\nu} = \bar{\mu}/\bar{\rho}_\infty$ denotes the kinematic shear viscosity. An often-used solution of equation (2.2) is the so-called Oseen vortex

$$\bar{v}_{Oseen}(r,t) = \frac{\bar{\Gamma}_\infty}{2\,\pi\,r}\left(1 - \mathrm{e}^{-r^2/(4\bar{\nu}t)}\right), \tag{2.3}$$

whose velocity profile decays as $1/r$ for large radii r. Partially differentiating (2.3) with respect to time t gives solutions of (2.2) that decay exponentially far outside the vortex core. Other solutions were found by Kirde (1962). They are given by

$$\bar{v}_{Kirde}(r,t) = \frac{\bar{v}(r_1,0)}{r_1^{\bar{n}}}\,\frac{\Gamma\left(\frac{1}{2}(\bar{n}+3)\right)\,2^{\bar{n}+1}}{4\,(\bar{\nu}t)^{(1-\bar{n})/2}}\,r\,M\left(\frac{1-\bar{n}}{2};2;-\frac{r^2}{4\bar{\nu}t}\right), \qquad -3 < \bar{n} < \infty. \tag{2.4}$$

$M(a;b;x)$ denotes the confluent hypergeometric function and $\Gamma(\bar{n})$ the factorial or Gamma function. For $t > 0$ the azimuthal velocity from equation (2.4) is proportional to the radius for $r \to 0$ and decays as $r^{\bar{n}}$ for large radii. Thus, only values $\bar{n} < 0$ are physically reasonable.

Experimental investigations of a single trailing vortex (Tung *et al.* 1983; see also the discussions in Moore & Saffman 1973 and Reinschke 1994) reveal that the azimuthal velocity profile resembles a Kirde vortex with $\bar{n} = -1/2$ for $r < l$ and an Oseen vortex outside. This distinction makes sense only if the vortex under consideration is

sufficiently 'young', i.e. $R < l$. In the experiments of Tung *et al.* (1983), l was found to be approximately $1/100$ of the wing span.

Compressible vortices are usually produced in flows of transonic convective speed, i.e. in transonic wind tunnels (Schürmann 1994) or in shock tubes (Mandella & Bershader 1987). These authors measure pressure and density profiles $\bar{p}(r) = \bar{p}(r, t_0)$ and $\bar{\rho}(r) = \bar{\rho}(r, t_0)$ simultaneously at a particular instant t_0 and determine the azimuthal velocity profile $\bar{v}(r) = \bar{v}(r, t_0)$ by means of the radial momentum equation

$$\frac{\bar{v}^2(r,t)}{r} = \frac{1}{\bar{\rho}(r,t)} \frac{\partial \bar{p}(r,t)}{\partial r}. \tag{2.5}$$

They find that *Lorentz functions* are the simplest best-fitting approximations to the measured pressure and density profiles, i.e.

$$\bar{p}(r) = \bar{p}_\infty \left(1 - \frac{t_p}{1 + (r/b_p)^2}\right), \qquad \bar{\rho}(r) = \bar{\rho}_\infty \left(1 - \frac{t_q}{1 + (r/b_q)^2}\right), \tag{2.6}$$

for radii r not greatly exceeding the vortex radius R. The constants $\bar{p}_\infty, \bar{\rho}_\infty, t_p, b_p, t_q$ and b_q are determined by comparison with the measured pressure and density curves. The azimuthal velocity $\bar{v}(r)$, which is computed from (2.6) and (2.5), resembles an Oseen vortex; $\bar{v}(r)$ decays as $1/r$ for $r \to \infty$.

Now we introduce non-dimensional variables. The non-dimensional radius x is defined via $r = xR$ and the non-dimensional sound speed $c(x)$ via $\bar{c}(r) = c(x)\bar{c}_\infty$. The non-dimensional base-flow variables are given as follows: the azimuthal velocity $V(x)$ via $\bar{v}(r) = V(x)\bar{c}_\infty$, the pressure $P(x)$ via $\bar{p}(r) = P(x)\bar{\rho}_\infty \bar{c}_\infty^2$, the density $Q(x)$ via $\bar{\rho}(r) = Q(x)\bar{\rho}_\infty$, the temperature $T(x)$ via $\bar{T}(r) = T(x)\bar{T}_\infty$, and the entropy $S(x)$ via $\bar{s}(r) - \bar{s}_\infty = S(x)\bar{R}^*$, where $\bar{R}^*$ is the specific gas constant. The subscript ∞ denotes base flow variables far outside the vortex core, where the medium is approximately at rest. The medium in which the vortex is formed is assumed to be an ideal gas, i.e. $\bar{c}_\infty^2 = \kappa \bar{p}_\infty / \bar{\rho}_\infty$, κ being the ratio of specific heats c_p/c_v.

A typical compressible vortex, as it was produced by Mandella & Bershader (1987) (see also Lee & Bershader 1994), is described in terms of non-dimensional variables by

$$P(x) = \frac{1}{\kappa}\left[1 - \frac{0.70}{1 + (x/1.25)^2}\right], \tag{2.7}$$

$$Q(x) = 1 - \frac{0.65}{1 + (x/1.5)^2}, \tag{2.8}$$

$$V(x) = \frac{0.947}{\kappa^{1/2}} x \left(1 + \left(x/1.25\right)^2\right)^{-1} \left(1 - \frac{0.65}{1 + \left(x/1.5\right)^2}\right)^{-1/2}. \tag{2.9}$$

Obviously, a single vortex of this kind could not exist alone since its kinetic energy would be infinite. Moreover, the scattered sound field of such a vortex does not converge because of the slow decay rate of the vortex far outside the vortex core. This phenomenon has been noted e.g. by Müller & Matschat (1959), O'Shea (1975) and Colonius *et al.* (1994). The 'remedy' is either to introduces a cut-off radius L, such that

$$V(x) \equiv 0, \qquad P(x) \equiv \frac{1}{\kappa}, \qquad Q(x) \equiv 1 \qquad \text{for} \qquad x > L,$$

or to use a modified vortex model that decays more rapidly in the far field, i.e. the far-field circulation of such a vortex would be zero. The introduction of a cut-off radius

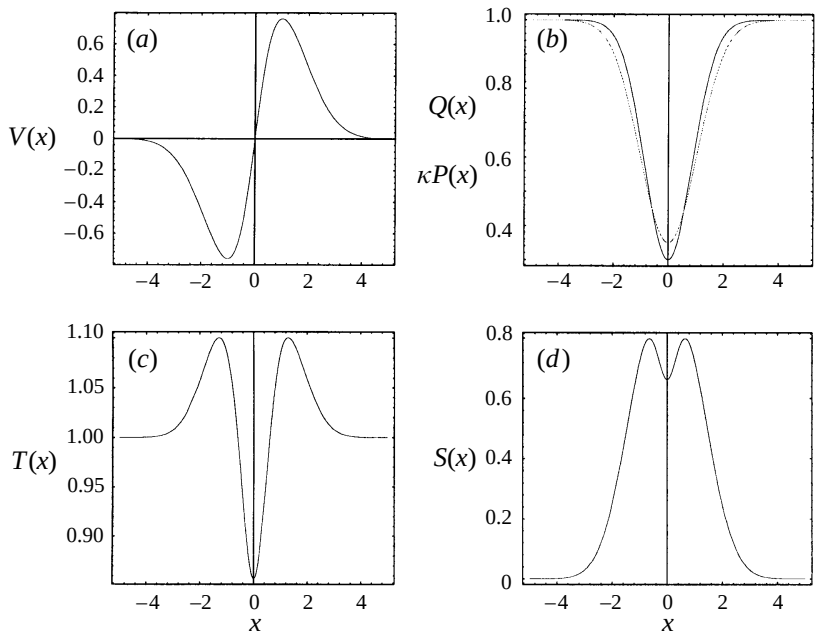

FIGURE 1. Non-dimensional base-flow functions of the model vortex: (*a*) velocity $V(x)$, (*b*) pressure $\kappa P(x)$ (solid) and density $Q(x)$ (dotted), (*c*) temperature $T(x)$, (*d*) entropy $S(x)$.

L is hard to justify physically, and the results of the corresponding sound-scattering theory would depend on the choice of L. In order to avoid this L-dependence, a modified vortex model was chosen which fits the experimental compressible vortex data of Mandella & Bershader (1987) in the core region, but decays exponentially outside:

$$P(x) = \frac{1}{\kappa}\left[1 - 0.70\mathrm{e}^{-c_r(a_x x)^2}\right], \tag{2.10}$$

$$Q(x) = 1 - 0.65\mathrm{e}^{-c_q(a_x x)^2}, \tag{2.11}$$

$$V(x) = \left(\frac{1.40c_r}{\kappa}\right)^{1/2} a_x x \mathrm{e}^{-(c_r - c_q)(a_x x)^2/2}\left(\mathrm{e}^{c_q(a_x x)^2} - 0.65\right)^{-1/2}, \tag{2.12}$$

where

$$c_r := \frac{\ln 2}{1.25^2}, \qquad c_q := \frac{\ln 2}{1.5^2}, \qquad \text{and} \qquad a_x := 1.23652.$$

The scaling factor a_x is determined such that $V_{max} = V(x = 1)$. Figure 1 shows the base-flow functions of the model vortex. For the model hot spot we set $P(x) \equiv 1/\kappa$ and $V(x) \equiv 0$. $Q(x)$ is the same as in (2.11).

3. Scattering of sound

From a theoretical point of view, the following two different kinds of scattering mechanisms can be distinguished.

(*a*) The medium in which the sound propagates is homogeneous and at rest. Obstacles are introduced into this medium, on the surface of which certain boundary conditions have to be satisfied. This can be achieved only if there exists a scattered wave in addition to the incoming wave.

(*b*) There are no obstacles and, thus, no boundary conditions within the medium in which the sound propagates. Instead, there is a base flow and/or inhomogeneities. A modified wave equation holds in the region of significant base flow; the asymptotic solution of the modified wave equation is again the sum of an incoming and a scattered/refracted wave.

The scattering of sound by a vortex is of the second kind. So is the quantum-mechanical scattering of plane waves by a central potential. Therefore, the authors have tried to apply quantum-mechanical scattering theory (phase-shift theory) to the acoustic scattering problem. Fetter (1964) has already followed this concept but considered only incompressible potential and Rankine vortices in the limit of very low frequencies $\bar{\omega}$.

3.1. *Basic equations*

The dimensional physical variables such as the pressure p_g, the density ρ_g and the velocity $\boldsymbol{v}_g = (u_g, v_g, w_g)$ are split into base-flow variables (denoted by a bar) and sound variables (dotted):

$$p_g = \bar{p} + \dot{p}, \quad \rho_g = \bar{\rho} + \dot{\rho}, \quad u_g = \dot{u}, \quad v_g = \bar{v} + \dot{v}, \quad w_g = \dot{w}.$$

Let the vortex be infinitely extended along the z-axis. Since plane sound waves with wave vector parallel to the z-axis are not scattered by the vortex (Fetter 1964), we can assume for simplicity that the wave vector is perpendicular to the vortex axis ($\dot{w} = 0$). Furthermore, we presume that all base-flow variables neither depend on the time t nor on the azimuthal angle ϕ during the scattering process. In general, friction and heat conduction will be neglected. The acoustic approximation is employed, i.e. all subsequent equations are linearized in the sound variables. The linearized Euler equations can be expressed as follows: the radial component is

$$\bar{\rho}\left[\left(\frac{\partial}{\partial t} + \frac{\bar{v}}{r}\frac{\partial}{\partial \phi}\right)\dot{u} - \frac{2\bar{v}}{r}\dot{v}\right] = -\frac{\partial \dot{p}}{\partial r} + \frac{\bar{v}^2}{r}\dot{\rho}, \tag{3.1}$$

and the azimuthal Euler equation yields

$$\bar{\rho}\left[\left(\frac{\partial}{\partial t} + \frac{\bar{v}}{r}\frac{\partial}{\partial \phi}\right)\dot{v} + \left(\frac{\mathrm{d}\bar{v}}{\mathrm{d}r} + \frac{\bar{v}}{r}\right)\dot{u}\right] = -\frac{1}{r}\frac{\partial \dot{p}}{\partial \phi}. \tag{3.2}$$

The linearized continuity equation is

$$\bar{\rho}\left(\frac{\partial}{\partial r} + \frac{1}{r}\right)\dot{u} + \frac{\bar{\rho}}{r}\frac{\partial \dot{v}}{\partial \phi} + \frac{\mathrm{d}\bar{\rho}}{\mathrm{d}r}\dot{u} = -\frac{\partial \dot{\rho}}{\partial t} - \frac{\bar{v}}{r}\frac{\partial \dot{\rho}}{\partial \phi}. \tag{3.3}$$

The sound perturbation is considered adiabatic. If the base flow is non-homentropic, the conservation of entropy takes the form

$$\frac{\partial \dot{p}}{\partial t} + \dot{u}\frac{\mathrm{d}\bar{p}}{\mathrm{d}r} + \bar{v}\frac{1}{r}\frac{\partial \dot{p}}{\partial \phi} = \bar{c}^2\left(\frac{\partial \dot{\rho}}{\partial t} + \bar{v}\frac{1}{r}\frac{\partial \dot{\rho}}{\partial \phi} + \dot{u}\frac{\mathrm{d}\bar{\rho}}{\mathrm{d}r}\right). \tag{3.4}$$

In the case of a homentropic base flow, i.e. $\operatorname{grad}\bar{s} = 0$, (3.4) reduces to

$$\dot{p} \approx \left.\frac{\partial p_g(\rho, s)}{\partial \rho_g}\right|_{\bar{s}} \dot{\rho} = \bar{c}^2(r)\dot{\rho},$$

or

$$\dot{p}(r, \phi, t) = \bar{c}^2(r)\dot{\rho}(r, \phi, t). \tag{3.5}$$

It turns out that there are no significant new difficulties arising if (3.4) is used instead of (3.5). Since we would like to avoid long formulas as much as possible, the scattering theory will be developed in §3 only for the homentropic case. Appendix B contains the corresponding formulas for general non-homentropic base flows.

The following separation assumption is made for all sound variables, written down here for $\dot{p}$ only:

$$\dot{p}(r,\phi,t) = \mathrm{Re}\left(\hat{p}_{\bar{\omega}}(r,\phi)\mathrm{e}^{-\mathrm{i}\bar{\omega}t}\right), \tag{3.6}$$

where $\hat{p}_{\bar{\omega}}(r,\phi)$ is a periodic function of the azimuthal coordinate ϕ:

$$\hat{p}_{\bar{\omega}}(r,\phi) = \hat{p}_{\bar{\omega}}(r,\phi+2\pi). \tag{3.7}$$

This allows us to develop $\hat{p}_{\bar{\omega}}(r,\phi)$ into a Fourier series:

$$\hat{p}_{\bar{\omega}}(r,\phi) = \sum_{n=-\infty}^{\infty} \hat{p}_{\bar{\omega}n}(r)\mathrm{e}^{\mathrm{i}n\phi} \tag{3.8}$$

with

$$\hat{p}_{\bar{\omega}n}(r) = \frac{1}{2\pi}\int_{\phi=0}^{2\pi} \mathrm{d}\phi\hat{p}_{\bar{\omega}}(r,\phi)\mathrm{e}^{-\mathrm{i}n\phi}. \tag{3.9}$$

Corresponding relations hold for all other acoustic variables.

By means of (3.5) we eliminate $\dot{\rho}(r,\phi,t)$ in (3.1) to (3.3) and apply $(1/2\pi)\int_{\phi=0}^{2\pi}\mathrm{d}\phi\mathrm{e}^{-\mathrm{i}n\phi}$ to these equations. This is equivalent to making the following substitutions in (3.1)–(3.3):

$$\frac{\partial}{\partial t} \longrightarrow -\mathrm{i}\bar{\omega}, \qquad \frac{\partial}{\partial\phi} \longrightarrow \mathrm{i}n, \qquad \dot{p}(r,\phi,t) \longrightarrow \hat{p}_{\bar{\omega}n}(r) \qquad \text{etc.,} \tag{3.10}$$

and the three equations then read

$$\bar{\rho}\left[\left(-\mathrm{i}\bar{\omega}+\frac{\bar{v}}{r}\mathrm{i}n\right)\hat{u}_{\bar{\omega}n} - \frac{2\bar{v}}{r}\hat{v}_{\bar{\omega}n}\right] = -\frac{\mathrm{d}\hat{p}_{\bar{\omega}n}}{\mathrm{d}r} + \frac{\bar{v}^2}{\bar{c}^2 r}\hat{p}_{\bar{\omega}n}, \tag{3.11}$$

$$\bar{\rho}\left[\left(-\mathrm{i}\bar{\omega}+\frac{\bar{v}}{r}\mathrm{i}n\right)\hat{v}_{\bar{\omega}n} + \left(\frac{\mathrm{d}\bar{v}}{\mathrm{d}r}+\frac{\bar{v}}{r}\right)\hat{u}_{\bar{\omega}n}\right] = -\mathrm{i}n\frac{1}{r}\hat{p}_{\bar{\omega}n}, \tag{3.12}$$

$$\bar{\rho}\left(\frac{\mathrm{d}}{\mathrm{d}r}+\frac{1}{r}\right)\hat{u}_{\bar{\omega}n} + \frac{\bar{\rho}}{r}\,\mathrm{i}n\hat{v}_{\bar{\omega}n} + \frac{\mathrm{d}\bar{\rho}}{\mathrm{d}r}\hat{u}_{\bar{\omega}n} = -\mathrm{i}\bar{\omega}\hat{\rho}_{\bar{\omega}n} - \frac{\bar{v}}{r}\,\mathrm{i}n\hat{\rho}_{\bar{\omega}n}. \tag{3.13}$$

Now we introduce non-dimensional sound variables which correspond to the non-dimensional base-flow variables defined in §2, below equation (2.6): the partial sound pressure wave $p_{\omega n}(x)$ is given by $\hat{p}_{\bar{\omega}n}(r) = p_{\omega n}(x)\bar{\rho}_\infty\bar{c}_\infty^2$, the partial sound density $\rho_{\omega n}(x)$ by $\hat{\rho}_{\bar{\omega}n}(r) = \rho_{\omega n}(x)\bar{\rho}_\infty$, the radial sound velocity component $u_{\omega n}(x)$ by $\hat{u}_{\bar{\omega}n}(r) = u_{\omega n}(x)\bar{c}_\infty$, and the azimuthal sound velocity component $v_{\omega n}(x)$ by $\hat{v}_{\bar{\omega}n}(r) = v_{\omega n}(x)\bar{c}_\infty$. For numerical calculations we assume that the sound propagates in an ideal, two-atomic gas. Thus,

$$c^2(x) = \kappa\frac{P(x)}{Q(x)}, \tag{3.14}$$

where $\kappa = 1.4$ is the ratio of specific heats. We introduce the following abbreviations:

$$\left.\begin{aligned} a_1(x) &:= \frac{V(x)\,n}{x} - \omega, \qquad & b_1(x) &:= \frac{2V(x)}{x}, \\ f_1(x) &:= \frac{\mathrm{d}V(x)}{\mathrm{d}x} + \frac{V(x)}{x}, \qquad & g_1(x) &:= \frac{V^2(x)}{c^2(x)x}. \end{aligned}\right\} \tag{3.15}$$

Now, the *basic equations* can be expressed as

$$\mathrm{i}\,Q\,a_1\,u_{\omega n} - Q\,b_1\,v_{\omega n} = -\frac{\mathrm{d}p_{\omega n}}{\mathrm{d}x} + g_1\,p_{\omega n}, \tag{3.16a}$$

$$Q\,f_1\,u_{\omega n} + \mathrm{i}\,Q\,a_1\,v_{\omega n} = -\mathrm{i}\,\frac{n}{x}\,p_{\omega n}, \tag{3.16b}$$

$$\frac{\mathrm{d}u_{\omega n}}{\mathrm{d}x} + \left(\frac{1}{x} + \frac{1}{Q}\frac{\mathrm{d}Q}{\mathrm{d}x}\right) u_{\omega n} + \mathrm{i}\,\frac{n}{x}\,v_{\omega n} = -\mathrm{i}\,\frac{1}{c^2\,Q}\,a_1\,p_{\omega n}. \tag{3.16c}$$

The system of equations corresponding to general non-homentropic vortices can be found in Appendix B, equations (B 1).

3.2. *The modified wave equation*

Equations (3.16) simplify drastically if there is no base flow. Elimination of $u_{\omega n}$ and $v_{\omega n}$ yields the separated normal wave equation in cylindrical coordinates

$$\frac{\mathrm{d}^2 p_{\omega n}}{\mathrm{d}x^2} + \frac{1}{x}\frac{\mathrm{d}p_{\omega n}}{\mathrm{d}x} + \left(k^2 - \frac{n^2}{x^2}\right) p_{\omega n} = 0 \tag{3.17}$$

with wavenumber $k := \omega/c$. In analogous fashion a modified wave equation (a second-order ordinary differential equation for $p_{\omega n}(x)$) can be constructed from the system (3.16). With the aid of (3.16*b*), we eliminate $v_{\omega n}$ from (3.16*a*) and (3.16*c*) and arrive at

$$p'_{\omega n} = \mathrm{i}\left(\frac{Q\,b_1\,f_1}{a_1} - Q\,a_1\right) u_{\omega n} + \left(g_1 - \frac{b_1\,n}{a_1\,x}\right) p_{\omega n}, \tag{3.18a}$$

$$u'_{\omega n} = \left(\frac{n\,f_1}{x\,a_1} - \frac{1}{x} - \frac{1}{Q}\,\frac{\mathrm{d}Q}{\mathrm{d}x}\right) u_{\omega n} - \mathrm{i}\left(\frac{a_1}{c^2\,Q} + \frac{n^2}{Q\,a_1\,x^2}\right) p_{\omega n}. \tag{3.18b}$$

Substituting (3.18*b*) into (3.18*a*) results in the *modified wave equation* for $p_{\omega n}(x)$

$$p''_{\omega n}(x) + co_1(x)p'_{\omega n}(x) + co_0(x)p_{\omega n}(x) = 0 \tag{3.19}$$

with

$$co_1(x) := \frac{1}{x} + \frac{n}{x}\frac{b_1(x)}{a_1(x)} - \frac{n}{x}\frac{f_1(x)}{a_1(x)} - g_1(x) + \frac{a'_1(x)}{a_1(x)} - \frac{a'_2(x)}{a_2(x)} \tag{3.20}$$

and

$$co_0(x) := \frac{-n^2}{x^2} - \frac{g_1(x)}{x} + \frac{n}{x}\frac{f_1(x)g_1(x)}{a_1(x)} - \frac{a_2(x)}{c^2(x)} - \frac{g_1(x)a'_1(x)}{a_1(x)} - \frac{n}{x}\frac{b_1(x)a'_2(x)}{a_1(x)a_2(x)} + \frac{g_1(x)a'_2(x)}{a_2(x)} - \frac{n}{x}\frac{b'_1(x)}{a_1(x)} - g'_1(x), \tag{3.21}$$

where $a_2 := b_1 f_1 - a_1^2$. The prime denotes $\mathrm{d}/\mathrm{d}x$. Equation (3.19) in conjunction with (3.20) and (3.21) reduces to the corresponding one obtained by Fetter (1964) if an incompressible potential vortex is considered. Note that equations (3.16) and (3.19) for a homentropic vortex depend only on two base-flow variables, namely $V(x)$ and $c^2(x)$, whereas in the general non-homentropic case a third, $Q(x)$, is required.

In general, equation (3.19) can be integrated numerically only. But before we can do this, some difficulties have to be overcome.

What are the initial values of $p_{\omega n}(x)$ and $p'_{\omega n}(x)$ for the integration in the neighbourhood of $x = 0$?

How can one integrate across the regular singularities of (3.19) at points $x \in (0, \infty)$?

These questions will be answered in the next subsection.

3.3. *Singularities*

3.3.1. *Singularity* $x_{s0} = 0$

We assume that all base-flow variables are regular functions of x in $x = 0$, i.e. they can be developed into power series. $V(x)$ has to be an odd function of x at $x = 0$, while $Q(x)$, $P(x)$ and $c^2(x)$ are even:

$$V(x) = \sum_{j=0}^{\infty} V_j\, x^{2j+1}, \qquad Q(x) = \sum_{j=0}^{\infty} Q_j\, x^{2j}, \qquad c^2(x) = \sum_{j=0}^{\infty} \tilde{c}_j\, x^{2j}. \tag{3.22}$$

As a consequence, $co_1(x)$ and $co_0(x)$ are of the form

$$co_1(x) =: \frac{1}{x}\left(1 + C_{11}x^2 + O(x^4)\right), \quad co_0(x) =: \frac{1}{x^2}\left((-n^2) + C_{01}x^2 + O(x^4)\right),$$

where the newly defined constants C_{11} and C_{01} can be expressed in terms of V_j, $\tilde{c}_j$, and – in the general case – Q_j. At least one fundamental solution of (3.19) in the vicinity of $x = 0$ can be found in terms of a Frobenius series

$$p_{\omega n}(x) = \sum_{j=0}^{\infty} p_j\, x^{j+v}. \tag{3.23}$$

Inserting (3.23) into (3.19) yields the index equation for v, namely $v(v-1)+v-n^2 = 0$, i.e. $v_1 = |n|$ and $v_2 = -|n|$. Since $v_1 - v_2 = 2|n| \in \mathcal{N}$, the second fundamental solution is not of the form (3.23). Just like Neumann functions (Bessel functions of the second kind), the second fundamental solution diverges at $x = 0$. Since all terms in the sum (3.8) are linearly independent, the sound pressure would be infinite at $x = 0$ if one $p_{\omega n}(x)$ diverged. Thus, the integration constant in front of the second fundamental solution has to be set equal to zero. The singularity at $x = 0$ caused by the cylindrical coordinate system yields one inner boundary condition for every partial wave $p_{\omega n}(x)$. The solution of (3.19) in the vicinity of $x = 0$ can be expressed as

$$p_{\omega n}(x) = x^n\left(p_0 + p_2x^2 + O(x^4)\right) \tag{3.24}$$

with

$$p_2 = -p_0\,\frac{C_{11}\,|n| + C_{01}}{4(|n|+1)},$$

where p_0 is an integration constant which can be chosen arbitrarily. We set $p_0 := 1$. In this way the initial values for the numerical integration of (3.18) and (3.19), respectively, are fixed.

3.3.2. *Singularity* x_{s2} *with* $a_2(x_{s2}) = 0$

This singularity only occurs in (3.19), but not in (3.18). Apart from the vicinity of x_{s1} with $a_1(x_{s1}) = 0$, we therefore use (3.18) for numerical integration.

3.3.3. *Singularity* x_{s1} *with* $a_1(x_{s1}) = 0$

This singularity cannot be so easily treated as the afore-mentioned one, since there is no system of two first-order differential equations similar to (3.18) where this singularity disappears. Fetter (1964) tried to get rid of it by a transformation of (3.19). The validity as well as the generalizability of his approach appear doubtful.

A close look at the singularity under consideration reveals that it is very similar to the kind that occurs in the stability analysis of a laminar, incompressible flow over a semi-infinite plate, i.e. the singularity in the Orr–Sommerfeld equation. The

neighbourhood of the singular point is called the *critical layer*. Let x_0 be the singular point of the Orr–Sommerfeld equation. A small imaginary part c_i is added to the real sound velocity $c = c_r$. The singular point is then translated from the real axis into the complex plane. If the sign of the imaginary part $\mathrm{Im}(x_0)$ of the singular point is positive (negative), the phase of $\eta := x - x_0$ is shifted by π ($-\pi$) when the real part of η is increased from negative to positive values and the limit $|\mathrm{Im}(x_0)| \longrightarrow 0$ is taken.

Generalizing the results on critical layers (Tollmien 1929, 1935, 1947; Lin 1955; Booker & Bretherton 1967) one concludes that the so-called *causal solution* is the correct one: the sign of c_i has to be chosen such that all acoustic perturbation variables vanish as $t \to -\infty$. In the following we will argue according to this causality criterion. It can be shown (see Appendix C) that the same results would have been obtained if friction had been taken into account instead of utilizing the causality argument.

The singularity x_{s1} occurs for

$$W(x_{s1}) := \frac{V(x_{s1})}{x_{s1}} = \frac{\omega}{n}. \tag{3.25}$$

Since $x \geqslant 0$, $V(x) \geqslant 0$, and $\omega \geqslant 0$, there are only singular points for partial waves $p_{\omega n}(x)$ with $n > 0$. Two cases have to be distinguished:

(a) $V(x)$ is 'predominantly linear' in x for small values of x, then $W(x)$ has its maximum at $x = 0$ and decays monotonically, i.e. $W'(x_{s1}) < 0$;

(b) $V(x)$ is proportional to a higher power of x for small x, e.g. $V(x) \sim x^3$. In this case $W(x)$ has its maximum value at a point $x > 0$. It is then possible that two different singularities occur at $x = x_{s1(1)}$ and $x = x_{s1(2)}$ with $W'(x_{s1(1)}) > 0$ and $W'(x_{s1(2)}) < 0$, respectively. (This case, however, appears to be of no physical significance since all known vortex models are of type (*a*).)

The separation of the time variable t was done via $\mathrm{e}^{-\mathrm{i}\omega t} = \mathrm{e}^{-\mathrm{i}\omega_r t}\,\mathrm{e}^{\omega_i t}$. A solution growing in time is thus obtained by setting $\omega_i > 0$. It is $W(\mathrm{Re}(x_{s1})) = \omega_r/n$. On the one hand we have

$$W(x_{s1}) = \frac{\omega}{n} = \frac{\omega_r}{n} + \mathrm{i}\,\frac{\omega_i}{n}$$

and, on the other hand, a Taylor-series expansion of $W(x_{s1})$ about $\mathrm{Re}(x_{s1})$ furnishes

$$W(x_{s1}) \approx W(\mathrm{Re}(x_{s1})) + W'(\mathrm{Re}(x_{s1}))\mathrm{i}\,\mathrm{Im}(x_{s1}).$$

It follows that

$$\mathrm{Im}(x_{s1}) \approx \frac{1}{W'(\mathrm{Re}(x_{s1}))}\,\frac{\omega_i}{n}, \tag{3.26}$$

i.e. for $W'(\mathrm{Re}(x_{s1})) < 0$ we have $\mathrm{Im}(x_{s1}) < 0$ (or for $W'(\mathrm{Re}(x_{s1})) > 0$ we get $\mathrm{Im}(x_{s1}) > 0$). This means: if x passes over the singular point x_{s1} from left to right and $|\omega_i|$ approaches zero, the argument θ changes from π (or $-\pi$) to 0, where $x - x_s = |x - x_s|\,\mathrm{e}^{\mathrm{i}\theta}$. Note once more that there are no vortex models known where type (*b*) singularities could occur.

From now on, the variables x_{s1} and ω are again assumed to be real. Let $I = [x_1, x_2]$ ($x_1 < x_{s1} < x_2$, $|x_1 - x_2| \ll 1$) be the *transition region* where we have to calculate the two fundamental solutions $p_{1\omega n}(x)$ and $p_{2\omega n}(x)$ of (3.19) in terms of power series. We first numerically integrate from the vicinity of $x = 0$ up to $x = x_1$, thus knowing $p_{\omega n}(x_1)$ and $p'_{\omega n}(x_1)$. The two integration constants IC_1 and IC_2 can be found by solving

$$\left.\begin{aligned} p_{\omega n}(x_1) &= IC_1 p_{1\omega n}(x_1) + IC_2 p_{2\omega n}(x_1), \\ p'_{\omega n}(x_1) &= IC_1 p'_{1\omega n}(x_1) + IC_2 p'_{2\omega n}(x_1). \end{aligned}\right\} \tag{3.27}$$

The integration is afterwards continued starting from x_2.

In order to obtain the two fundamental solutions around x_{s1}, we proceed in a similar way as in §3.3.1. The coefficients $co_1(x)$ and $co_0(x)$ are developed into power series:

$$co_1(x) = \frac{1}{x - x_{s1}} \sum_{j=0}^{\infty} \alpha_j (x - x_{s1})^j, \quad co_0(x) = \frac{1}{(x - x_{s1})^2} \sum_{j=0}^{\infty} \beta_j (x - x_{s1})^j, \tag{3.28}$$

where α_j and β_j are constants. In doing this, it turns out that the base flow of a potential vortex is a special case which has to be treated separately since zeros of $a_1(x)$ and $a_2(x)$ coincide. This case was considered by Fetter (1964). For technical reasons we want to exclude it in the subsequent discussion. It then follows from (3.21) that $\beta_0 = 0$ while (3.20) yields $\alpha_0 = n(b_1(x) - f_1(x)) / \left(x a_1'(x)\right) + 1$, which turns out to be equal to zero, too, if use is made of the definitions (3.15). Writing $p_{\omega n}(x)$ as a Frobenius series

$$p_{\omega n}(x) = \sum_{j=0}^{\infty} c_j (x - x_{s1})^{j+v} \tag{3.29}$$

leads to the index equation $v(v-1) = 0$, i.e. $v_1 = 1$ and $v_2 = 0$. Thus, the first fundamental solution assumes the form

$$p_{1\omega n}(x) = \sum_{j=0}^{\infty} c_j (x - x_{s1})^{j+1} \tag{3.30}$$

with

$$c_0 := 1, \qquad c_j := -\frac{\sum_{k=1}^{j} c_{j-k} (\beta_k + \alpha_k (j + 1 - k))}{(j+1)\, j}, \qquad j = 1, 2, \ldots .$$

Since $v_1 - v_2 = 1$, the second fundamental solution is usually not a Frobenius series. This solution, $p_{2\omega n}(x)$, can be found by setting

$$p_{2\omega n}(x) = u_p(x) p_{1\omega n}(x). \tag{3.31}$$

One obtains

$$u_p'(x) = \left(\sum_{j=0}^{\infty} c_j (x - x_{s1})^{j+1} \right)^{-2} \exp\left(-\sum_{j=1}^{\infty} \frac{1}{j} \alpha_j (x - x_{s1})^j \right) =: (x - x_{s1})^{-2} g(x) \tag{3.32}$$

with

$$g(x) =: \sum_{j=0}^{\infty} g_j (x - x_{s1})^j,$$

where the g_j are newly defined constants. In particular, we have

$$g_0 = \frac{1}{c_0^2} = 1, \qquad g_1 = -\frac{\alpha_1}{c_0^2} - 2\frac{c_1}{c_0^3} = \frac{\beta_1}{c_0^2} = \beta_1 \neq 0.$$

Integrating (3.32) yields

$$u_p(x) = -(x - x_{s1})^{-1} + \beta_1 \ln(x - x_{s1}) + \sum_{j=1}^{\infty} \frac{1}{j} g_{j+1} (x - x_{s1})^j, \tag{3.33}$$

and together with (3.30) and (3.31) the second fundamental solution is found. Note

that the logarithmic term in $p_{2\omega n}(x)$ does not vanish. This logarithmic term in (3.33) stands for $\ln|x - x_{s1}|$ for $x < x_{s1}$ and for $\ln|x - x_{s1}| \mp i\pi$ for $x > x_{s1}$, whereby the minus sign applies for a type (*a*) and the plus sign for a type (*b*) singularity.

In the non-homentropic base flow case, $\alpha_0 = 0$ is maintained, but $\beta_0 = 0$ is no longer valid. As a consequence, ν_1 and ν_2 as well as their difference are not integers, thus allowing both fundamental solutions of (3.19) to be expressed as Frobenius series

$$p_{i,\omega n}(x) = (x - x_{s1})^{\nu_i} \sum_{j=0}^{\infty} c_{i,j}\,(x - x_{s1})^j, \qquad (i = 1, 2) \tag{3.34}$$

where

$$c_{i,0} = 1, \qquad c_{i,j} = -\frac{\sum_{k=1}^{j} c_{i,j-k}\,(\beta_k + \alpha_k\,(j - k + \nu_i))}{(j + \nu_i)\,(j - 1 + \nu_i) + \beta_0}, \quad j = 1, 2, \ldots . \tag{3.35}$$

The expression $(x - x_{s1})^{\nu_i}$ means $|x - x_{s1}|^{\nu_i}$ for $x < x_{s1}$ and $|x - x_{s1}|^{\nu_i} e^{\mp i\pi\nu_i}$ for $x > x_{s1}$ with the minus sign for a type (*a*) and the plus sign for a type (*b*) singularity.

Finally in this subsection we want to investigate the physical significance of the singularities under consideration. If there were no energy transfer between the base flow and the sound perturbation, the integral

$$\langle E_s \rangle_t := \left\langle \int_{\mathscr{C}} \mathrm{d}\boldsymbol{x} \cdot \boldsymbol{I}_s \right\rangle_t = \int_{\mathscr{C}} \mathrm{d}\boldsymbol{x} \cdot \tfrac{1}{2}\,\mathrm{Re}\,(\boldsymbol{v}_\omega(x, \phi) p_\omega(x, \phi)) \tag{3.36}$$

would have to vanish. $\mathscr{C}$ symbolizes a closed contour encircling the vortex in the (x, ϕ)-plane. The brackets $\langle . \rangle_t$ represent averaging in time. $\boldsymbol{I}_s$ is the energy flux or the total acoustic intensity, i.e. the intensity of both incoming and scattered sound waves. If the ratio $p'_{\omega n}(x)/p_{\omega n}(x)$ is real for all integer n and sufficiently large x, $\langle E_s \rangle_t$ is definitely equal to zero. But if the pressure ratio is complex for some n, $\langle E_s \rangle_t$ will in general be different from zero. Since the non-dimensional azimuthal velocity $V(x)$ in a vortex does not vanish everywhere, there is a number $n_{min} > 0$ such that

$$\forall \quad n \geqslant n_{min} \quad \exists \quad x_{s1}(n) : \quad a_1(x_{s1}(n)) = 0.$$

The occurrence of a singularity at $x = x_{s1}(n)$ causes the ratio $p'_{\omega n}(x)/p_{\omega n}(x)$ to be complex for $x > x_{s1}(n)$ and, hence, the integral in (3.36) might be non-zero. This can be interpreted in a way analogous to McKenzie (1979): the critical layer causes an energy transfer between the base flow and the acoustic perturbation.

If $V(x) \equiv 0$, i.e. if we consider the scattering of sound by a cylindrical inhomogeneity, there are no singularities and, thus, there is no energy transfer. Since scattering processes without energy transfer are usually referred to as *elastic* scattering processes, we will call the scattering by an inhomogeneity *elastic scattering* and that by a vortex *inelastic scattering*.

3.4. *Scattering theory*

Utilizing the theory developed in §3.3, we can compute the partial waves $p_{\omega n}(x)$ up to an arbitrary scaling factor which was called p_0 and set equal to one. These partial waves contain the incoming as well as the scattered sound wave. It is the aim of this subsection to derive an expression for the far-field scattered sound wave alone, provided that the amplitude of the incoming plane sound wave is known.

A three-dimensional elastic scattering theory for plane waves scattered by a real

central potential has been developed in quantum mechanics (see e.g. Taylor 1972). This theory is generally referred to as *phase-shift method*. It could be directly transferred to the two-dimensional sound scattering problem if there were no singularities of the kind treated in §3.3.3. If a partial wave possesses such a singularity and the ratio $p'_{\omega n}(x)/p_{\omega n}(x)$ is thus complex outside the vortex region, two real phase angles (instead of one in the elastic quantum-mechanical scattering theory) are required to describe one partial wave.

The partial wave $p_{\omega n}(x)$ is a solution of the Bessel differential equation (3.17) for large x, i.e. ($\omega = k$ (!)):

$$\begin{aligned} p_{\omega n}(x) &= A_n J_n(kx) + B_n Y_n(kx) \\ &\xrightarrow{x\to\infty} \left(\frac{2}{\pi kx}\right)^{1/2} \left[A_n \cos\left(kx - \frac{\pi n}{2} - \frac{\pi}{4}\right) + B_n \sin\left(kx - \frac{\pi n}{2} - \frac{\pi}{4}\right)\right] \end{aligned} \tag{3.37}$$

with complex constants A_n and B_n. These constants are numerically evaluated by solving

$$\begin{pmatrix} p_{\omega n}(x) \\ p'_{\omega n}(x) \end{pmatrix}_{x=x_f} = \begin{pmatrix} J_n(kx) & Y_n(kx) \\ k\,\dfrac{\mathrm{d}}{\mathrm{d}(kx)} J_n(kx) & k\,\dfrac{\mathrm{d}}{\mathrm{d}(kx)} Y_n(kx) \end{pmatrix}_{x=x_f} \begin{pmatrix} A_n \\ B_n \end{pmatrix}, \tag{3.38}$$

where x_f is chosen sufficiently large. For the solutions A_n, B_n to converge for sufficiently large x_f, the base flow of the model vortex has to decay rapidly enough far outside the vortex core. This is ensured by the base-flow variables as prescribed by (2.10)–(2.12). We define new constants $\tilde{A}_n$ and $\tilde{B}_n$ via $A_n =: \tilde{A}_n(1 + \mathrm{i})$ and $B_n/\tilde{A}_n =: \tilde{B}_n =: \tilde{B}_{rn} + \mathrm{i}\tilde{B}_{in}$. Substituting A_n and B_n in the second line of (3.37) results in

$$p_{\omega n}(x) \xrightarrow{x\to\infty} \frac{1}{(kx)^{1/2}} \left[N_{rn} \cos\left(kx - \frac{\pi n}{2} - \frac{\pi}{4} + \delta_{rn}\right) + \mathrm{i}\, N_{in} \cos\left(kx - \frac{\pi n}{2} - \frac{\pi}{4} + \delta_{in}\right)\right] \tag{3.39}$$

with

$$\delta_{rn} := \arctan\left(-\tilde{B}_{rn}\right), \qquad \delta_{in} := \arctan\left(-\tilde{B}_{in}\right) \tag{3.40}$$

and

$$N_{rn} := \tilde{A}_n \left(\frac{2}{\pi}\right)^{1/2} \left(1 + \tilde{B}_{rn}^2\right)^{1/2}, \qquad N_{in} := \tilde{A}_n \left(\frac{2}{\pi}\right)^{1/2} \left(1 + \tilde{B}_{in}^2\right)^{1/2}. \tag{3.41}$$

If there were no vortex, we would obtain

$$p_{\omega n}(x) = C_n J_n(kx) \xrightarrow{x\to\infty} (C_{rn} + \mathrm{i}\, C_{in}) \left(\frac{2}{\pi kx}\right)^{1/2} \cos\left(kx - \frac{\pi n}{2} - \frac{\pi}{4}\right), \tag{3.42}$$

i.e. the essential influence of the base flow is that it causes a phase shift of all partial waves with two phase angles δ_{rn} and δ_{in} for each partial wave. If a $p_{\omega n}(x)$ is multiplied by an arbitrary complex constant, this has no impact on the phase shifts. The phase angles are, thus, independent of the special value of p_0 in (3.24), which had been set equal to 1 arbitrarily. The aim is therefore to express the required solution for the scattered wave in terms of the phase angles only, as it is done in quantum-mechanical scattering theory.

We have $p'_{\omega n}(x)/p_{\omega n}(x) \in \mathscr{R} \leftrightarrow A_n/B_n \in \mathscr{R}$. If $p'_{\omega n}(x)/p_{\omega n}(x) \in \mathscr{R}$, the phase shift of this partial wave can be described by one phase angle δ_n, since $\delta_{rn} = \delta_{in} =: \delta_n$ holds

in this case. The scattering theory is thus much simpler if we restrict ourselves to the scattering by inhomogeneities.

The Fourier component of the sound pressure

$$p_\omega(x,\phi) = \sum_{n=-\infty}^{\infty} p_{\omega n}(x)\mathrm{e}^{\mathrm{i}n\phi} \tag{3.43}$$

can be decomposed into a sum of an incoming wave $p_\omega^{in}(x,\phi)$ and a scattered wave $p_\omega^{sc}(x,\phi)$. The incoming plane wave can be developed into a series of Bessel functions of the first kind $J_n(kx)$ (see Morse & Feshbach 1953):

$$\begin{aligned} p_\omega^{in}(x,\phi) &= F\mathrm{e}^{\mathrm{i}\boldsymbol{k}\cdot\boldsymbol{x}} = F\mathrm{e}^{\mathrm{i}kx\cos\phi} = \sum_{n=-\infty}^{\infty} FJ_n(kx)\mathrm{e}^{\mathrm{i}n(\phi+\pi/2)} \\ &\xrightarrow{x\to\infty} \sum_{n=-\infty}^{\infty} F\left(\frac{2}{\pi kx}\right)^{1/2} \cos\left(kx-\frac{\pi n}{2}-\frac{\pi}{4}\right)\mathrm{e}^{\mathrm{i}n(\phi+\pi/2)}, \end{aligned} \tag{3.44}$$

where the complex amplitude $F = F_r + \mathrm{i}F_i$ determines magnitude and phase of the incoming plane wave. The scattered wave has to satisfy the Helmholtz equation

$$\Delta p_\omega^{sc}(x,\phi) + k^2\, p_\omega^{sc}(x,\phi) = 0 \tag{3.45}$$

as well as Sommerfeld's radiation condition

$$\lim_{x\to\infty} x^{1/2}\left(\frac{\partial p_\omega^{sc}}{\partial x} - \mathrm{i}kp_\omega^{sc}\right) = 0. \tag{3.46}$$

Therefore the scattered wave asymptotically is

$$p_\omega^{sc}(x,\phi) \xrightarrow{x\to\infty} F\, x^{-1/2}\, f(\phi)\ \mathrm{e}^{\mathrm{i}kx+\mathrm{i}\pi/4}, \tag{3.47}$$

where $f(\phi)$ is called the *scattering amplitude*. On the one hand (3.44) and (3.47) yield

$$p_\omega(x,\phi) = p_\omega^{in}(x,\phi) + p_\omega^{sc}(x,\phi),$$

i.e.

$$\begin{aligned} p_\omega(x,\phi) \xrightarrow{x\to\infty} \sum_{n=-\infty}^{\infty} F\left(\frac{2}{\pi kx}\right)^{1/2} &\cos\left(kx-\frac{\pi n}{2}-\frac{\pi}{4}\right)\mathrm{e}^{\mathrm{i}n(\phi+\frac{\pi}{2})} \\ &+ F\, x^{-1/2}\, f(\phi)\ \mathrm{e}^{\mathrm{i}kx+\mathrm{i}\pi/4}, \end{aligned} \tag{3.48}$$

and on the other hand it is deduced from (3.39) and (3.43) that

$$\begin{aligned} p_\omega(x,\phi) \xrightarrow{x\to\infty} \sum_{n=-\infty}^{\infty} &\frac{1}{(kx)^{1/2}}\left\{N_{rn}\cos\left(kx-\frac{\pi n}{2}-\frac{\pi}{4}+\delta_{rn}\right)\right\}\mathrm{e}^{\mathrm{i}n\phi} \\ &+ \mathrm{i}\,\frac{1}{(kx)^{1/2}}\left\{N_{in}\cos\left(kx-\frac{\pi n}{2}-\frac{\pi}{4}+\delta_{in}\right)\right\}\mathrm{e}^{\mathrm{i}n\phi}. \end{aligned} \tag{3.49}$$

Equation (3.49) can be transformed into

$$\begin{aligned} p_\omega(x,\phi) = \sum_{n=-\infty}^{\infty} &\left(\frac{2}{\pi kx}\right)^{1/2}\cos\left(kx-\frac{\pi n}{2}-\frac{\pi}{4}\right)\left(\frac{\pi}{2}\right)^{1/2}\mathrm{e}^{\mathrm{i}n\phi}\left(N_{rn}\mathrm{e}^{-\mathrm{i}\delta_{rn}} + \mathrm{i}N_{in}\mathrm{e}^{-\mathrm{i}\delta_{in}}\right) \\ &+ x^{-1/2}\,\mathrm{e}^{\mathrm{i}kx+\mathrm{i}\pi/4}\sum_{n=-\infty}^{\infty} k^{-1/2}\ \mathrm{e}^{\mathrm{i}n\phi}\,\mathrm{e}^{-\mathrm{i}\pi n/2}\ (N_{rn}\sin\delta_{rn} + \mathrm{i}\,N_{in}\sin\delta_{in}). \end{aligned} \tag{3.50}$$

A comparison of the upper lines of (3.48) and (3.50) gives

$$F \cdot \mathrm{e}^{\mathrm{i}n\pi/2} = \left(\frac{\pi}{2}\right)^{1/2} \left(N_{rn}\,\mathrm{e}^{-\mathrm{i}\delta_{rn}} + \mathrm{i}N_{in}\,\mathrm{e}^{-\mathrm{i}\delta_{in}}\right). \tag{3.51}$$

This provides, together with (3.41), an expression for the so far unknown constants $\tilde{A}_n$:

$$\tilde{A}_n = F\mathrm{e}^{\mathrm{i}\,\pi n/2} \Bigg/ \left(\frac{\mathrm{e}^{-\mathrm{i}\delta_{rn}}}{\cos\delta_{rn}} + \mathrm{i}\,\frac{\mathrm{e}^{-\mathrm{i}\delta_{in}}}{\cos\delta_{in}}\right). \tag{3.52}$$

Comparing the lower lines of (3.48) and (3.50) gives a formula for the inelastic scattering amplitude:

$$f^{inel}(\phi) = \sum_{n=-\infty}^{\infty} F^{-1}\,k^{-1/2}\,\mathrm{e}^{\mathrm{i}n\phi}\,\mathrm{e}^{-\mathrm{i}\pi n/2}\,(N_{rn}\sin\delta_{rn} + \mathrm{i}\,N_{in}\sin\delta_{in}). \tag{3.53}$$

Finally, we insert (3.41) and (3.52) into (3.53) and arrive at

$$f^{inel}(\phi) = \left(\frac{2}{\pi k}\right)^{1/2} \sum_{n=-\infty}^{\infty} \mathrm{e}^{\mathrm{i}n\phi}\,(\tan\delta_{rn} + \mathrm{i}\,\tan\delta_{in}) \Bigg/ \left(\frac{\mathrm{e}^{-\mathrm{i}\delta_{rn}}}{\cos\delta_{rn}} + \mathrm{i}\,\frac{\mathrm{e}^{-\mathrm{i}\delta_{in}}}{\cos\delta_{in}}\right). \tag{3.54}$$

If the scattering is elastic, $\delta_{in} = \delta_{rn} =: \delta_n$, and equation (3.54) reduces to

$$f^{el}(\phi) = \left(\frac{2}{\pi k}\right)^{1/2} \sum_{n=-\infty}^{\infty} \mathrm{e}^{\mathrm{i}n\phi}\,\mathrm{e}^{\mathrm{i}\,\delta_n}\,\sin\delta_n. \tag{3.55}$$

From an experimental point of view, one is usually interested in the differential cross-section and the total cross-section, i.e.

$$\frac{d\sigma_S}{d\phi}(\phi) = |f(\phi)|^2 \qquad \text{and} \qquad \sigma_S = \int_0^{2\pi} |f(\phi)|^2\,\mathrm{d}\phi, \tag{3.56}$$

instead of the scattering amplitude itself. The differential cross-sections for several values of k are plotted for scattering by the model vortex (figure 2) as well as for scattering by the model inhomogeneity (figure 3). Note that in the latter case the elastic scattering amplitudes and, consequently, the differential cross-sections are even functions of ϕ. This is guaranteed by $\delta_n = \delta_{(-n)}$, which itself is a consequence of the fact that the modified wave equation contains only even powers of n for an elastic scattering process.

The total cross-section tends towards zero for $\omega \to 0$. Let us, as usual, call the $(n = 0)$-term in (3.54) and (3.55) the *monopole term*, the $(|n| = 1)$-terms the *dipole terms* etc. What are the dominating terms in the low-frequency or long-wavelength limit? For the numerically tested model vortex, the monopole, dipole and quadrupole terms are prevailing, whereas in the case of the model hot spot only the dipole term has to be taken into account. (The latter result is of no surprise as it had already been predicted by Rayleigh 1945.) More and more higher-order multipole terms have to be taken into account the higher the frequency of the incoming sound wave. This will be looked at in greater detail in the next subsection.

3.5. *Formal analogy between quantum-mechanical and acoustic scattering theory*

All equations that will subsequently be quoted from quantum mechanics will be denoted by $\stackrel{*}{=}$ instead of $=$ in order to avoid confusion between quantum-mechanical and acoustic theories.

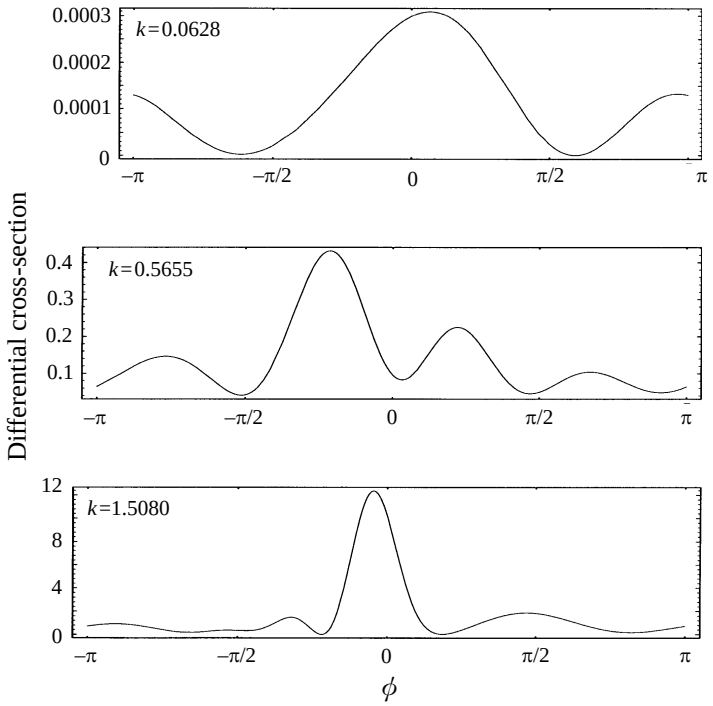

FIGURE 2. Differential cross-sections for the sound scattering by the model vortex for different wavenumbers k.

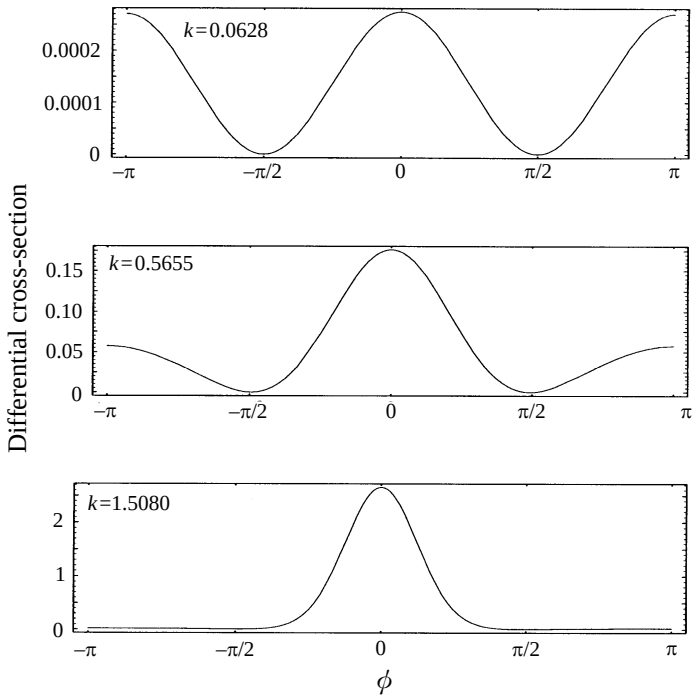

FIGURE 3. Differential cross-sections for the sound scattering by the model hot spot for different wavenumbers k.

The elastic total cross-section is given by

$$\sigma_S^{el} = \frac{4}{\omega} \sum_{n=-\infty}^{\infty} \sin^2 \delta_n.$$

Within the quantum-mechanical elastic scattering theory one obtains for the same variable

$$\sigma_S^{el} \stackrel{*}{=} \frac{4\pi}{p^2} \sum_{l=0}^{\infty} (2l+1) \sin^2 \delta_l,$$

which indicates that there is some formal correspondence between quantum-mechanical and acoustic scattering variables, e.g. $\delta_l \hat{=} \delta_n$. In order to support this assertion, we rewrite equation (3.19) as

$$p''_{\omega n}(x) + \left(\frac{1}{x} - \tilde{co}_1(x)\right) p'_{\omega n}(x) + \left(\omega^2 - \frac{n^2}{x^2} - \tilde{co}_0(x)\right) p_{\omega n}(x) = 0, \tag{3.57}$$

where the coefficient functions $\tilde{co}_1(x)$ and $\tilde{co}_0(x)$ are less singular at $x = 0$ than the dominant terms $1/x$ and n^2/x^2, respectively. The term proportional to $p'_{\omega n}(x)$ can be eliminated by a transformation $p_{\omega n}(x) \mapsto \varphi_{\omega n}(x)$ via

$$p_{\omega n}(x) = \varphi_{\omega n}(x) \exp\left(-\frac{1}{2} \int_1^x \left(\frac{1}{\xi} - \tilde{co}_1(\xi)\right) \mathrm{d}\xi\right)$$

which replaces (3.57) by

$$\varphi''_{\omega n}(x) + \left(\omega^2 - \frac{n^2 - \frac{1}{4}}{x^2} - C_{\omega n}(x)\right) \varphi_{\omega n}(x) = 0, \tag{3.58}$$

where $C_{\omega n}(x)$ is defined as

$$C_{\omega n}(x) := \tilde{co}_0(x) + (\tilde{co}_1(x))^2 - \tfrac{1}{2} \tilde{co}'_1(x) - \frac{1}{2} \frac{\tilde{co}_1(x)}{x}.$$

The radial Schrödinger equation for the quantum-mechanical partial wave functions $\psi_l(r)$ is (cf. e.g. Taylor 1972)

$$\psi''_l(r) + \left(p^2 - \frac{l(l+1)}{r^2} - V(r)\right) \psi_l(r) \stackrel{*}{=} 0,$$

or, if l is replaced by $\lambda := l + \frac{1}{2}$,

$$\psi''_l(r) + \left(p^2 - \frac{\lambda^2 - \frac{1}{4}}{r^2} - V(r)\right) \psi_l(r) \stackrel{*}{=} 0. \tag{3.59}$$

Here, r stands for the distance from the origin in $\mathscr{R}^3$, $V(r)$ is the quantum-mechanical central potential, l is the angular momentum eigenvalue, and p the momentum eigenvalue of the incoming particle. The comparison of (3.59) and (3.58) suggests a correspondence as listed in table 1. By means of a simple energy argument (cf. Taylor 1972) one concludes in quantum mechanics that phase angles δ_l with

$$l \gg p a_V$$

(a_V is the typical extension of the scattering potential) do not contribute significantly to the scattering amplitude. Utilizing the above-mentioned analogy, we suppose that

Quantum-mechanical variable	Acoustic variable	Correspondence
three-dimensional radius: r	two-dimensional radius: x	$r \hat{=} x$
particle momentum eigenvalue: p	frequency of the incoming wave: ω	$p \hat{=} \omega$
angular momentum eigenvalue: l	separation parameter for the azimuthal angle ϕ: n	$n \hat{=} l + \frac{1}{2}$
central potential: $V(r)$	potential function: $C_{\omega n}(x)$	$V(r) \hat{=} C_{\omega n}(x)$
phase angle: δ_l	phase angle: δ_n	$\delta_l \hat{=} \delta_n$
partial wave function: $\psi_l(r)$	transf. partial sound pressure: $\varphi_{\omega n}(x)$	$\psi_l(r) \hat{=} \varphi_{\omega n}(x)$

TABLE 1. The correspondence between quantum-mechanical and acoustic scattering variables

in the acoustic case those phase angles δ_n with

$$|n| \gg \omega a_C \tag{3.60}$$

(a_C is a typical extension of the vortex/hot spot) are negligible. This result is confirmed by numerical experiments according to which the number of phase shifts to be taken into account grows linearly with frequency ω.

4. Application of the scattering theory

4.1. *Shocks and N-waves*

A periodic sequence of shocks is approximated by a sequence of N-waves (see figure 4). The steep flanks represent the shocks with a finite period of time τ_S of increasing pressure. The time τ_A during which the pressure decreases between two successive shocks should be long in comparison to τ_S. Such shock N-waves with a sufficiently small amplitude can be decomposed into a Fourier series (for practical calculations a Fourier sum) of sinusoidal sound waves of different frequencies. Shock–vortex interaction can thus be theoretically treated by an appropriate sound-scattering theory if weak shocks only are considered. Vortex deformation should be negligible during the passage of a shock. We should therefore consider a strong vortex, regarding the base flow as compressible. In the same way shock–hot-spot interaction can be theoretically investigated. In addition to the non-dimensional polar coordinate system (x, ϕ), we will use non-dimensional Cartesian coordinates (ξ_1, ξ_2) when it is appropriate.

4.2. *Shock–vortex interaction*

In our calculations the ratio τ_A/τ_S was chosen to be 24 and also 24 different frequencies were retained in the Fourier sum. The distance between two successive shock fronts was 100 times the vortex radius R. The vortex rotated in an anti-clockwise direction.

Experimental investigations of the shock–vortex interaction have mainly been carried out in shock tubes (e.g. Hollingsworth & Richards 1955; Dosanjh & Weeks 1965). A plane shock passes over a two-dimensional wing at a small angle of attack. Thereby a cylindrical vortex is shed from the trailing edge of the wing. The shock is reflected at the closed end of the shock tube and interacts with the vortex afterwards. These experiments reveal the following three different phenomena related to shock–vortex interaction.

1. The shock is deformed whilst passing over the vortex. Depending on the shock

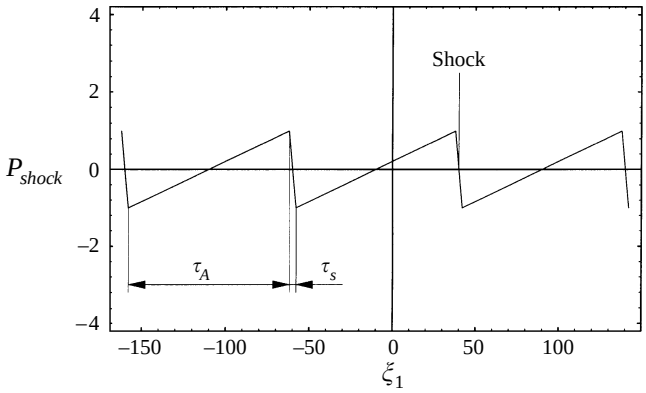

FIGURE 4. A periodic sequence of shocks represented by successive N-waves.

and vortex strengths, this can result in structures of 'initial' and 'reflected' shocks as they are known from the reflection of a plane shock by a wedge (see Elzey, Picone & Oran 1992).

2. A cylindrical sound wave with a quasi-quadrupolar amplitude is formed, which is cut off by the shock since the sound velocity exceeds the shock velocity in the centre-of-vortex coordinate system. The predominantly quadrupolar directivity pattern of the cylindrical sound wave is particularly well documented in Dosanjh & Weeks (1965 see, in particular, figure 4). The authors were able to measure the pressure amplitude along the circumference of the cylindrical sound wave very accurately and fitted a curve consisting of monopole, dipole and quadrupole terms only to their experimental data. The fit is very good, and Dosanjh & Weeks (1965) find the quadrupole term to be the dominant one.

3. The vortex is deformed.

It is the second phenomenon which is supposed to be fairly well described by the sound-scattering theory. Apart from this, one could hope that the calculated scattered sound signal also contains a structure which can be interpreted as a 'reflected shock'. The third phenomenon, apparently, cannot be treated.

The spatial pressure distribution of the scattered sound signal for the model vortex is shown in figure 5 as a so-called 'density plot'. Brighter up to white spots represent areas of positive sound pressure and darker up to black spots indicate negative sound pressures, respectively. Zero pressure corresponds to grey. The cross in the middle of the graphs marks the centre of the vortex. The position of the undisturbed incoming shock, which has passed over the vortex, is drawn in by three lines. The left one at $\xi_1 = 38$ corresponds to a pressure maximum of the N-wave, the right one at $\xi_1 = 42$ to a pressure minimum and the line in the middle at $\xi_1 = 40$ is where the pressure crosses the zero value. In an inner region, for $x < 15$, the scattered sound pressure was set equal to zero because the calculated signal is only asymptotically valid.

The kind of representation chosen in figure 5(*a*) emphasizes structures caused by small pressure fluctuations in an exaggerated manner. These small fluctuations are probably the result of the finite Fourier sum and have no physical meaning. In figure 5(*b*) they are made disappear by a different kind of representation. Although the main structure is still quite complicated, a quadrupole-like nearly cylindrical sound wave might now be discernible where a circle is additionally drawn on the figure. In the calculated picture, the cylindrical sound wave forms a full circle because sound and shock speeds are equal in the weak shock limit. The location of the positive and

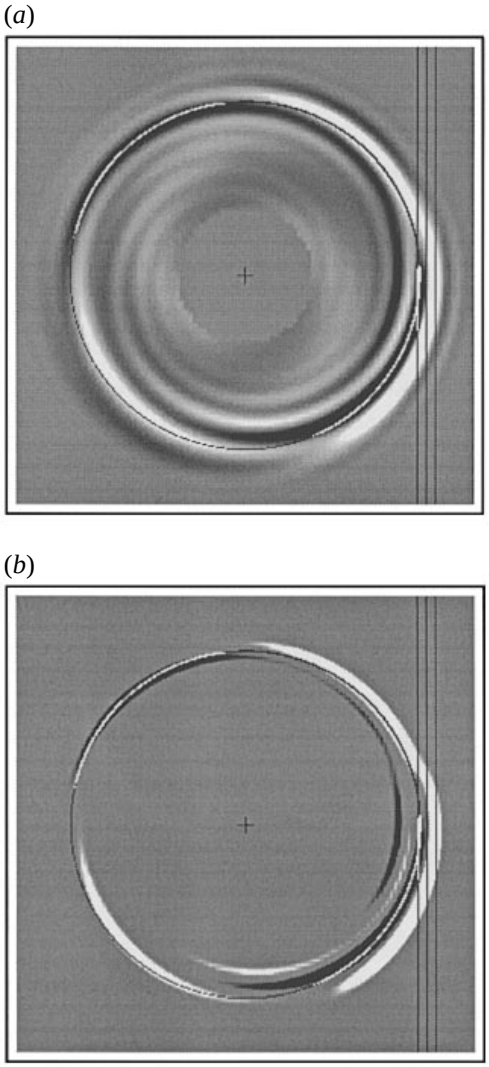

FIGURE 5. Density plot of the scattered sound pressure signal for the scattering by the model vortex.

negative pressure peaks is consistent with experimental findings of Hollingsworth & Richards (1955) and Dosanjh & Weeks (1965). A quantitative comparison of the amplitude of the scattered sound wave between Dosanjh & Weeks' experiments and this theoretical result is, however, not possible because their shocks were not weak in the sense of this theory. The white area in the fourth quadrant might tentatively be interpreted as a reflected shock.

4.3. *Shock–hot-spot interaction*

For the computed shock–hot-spot interaction we used the model hot spot of §2 as well as the N-wave model of §4.2.

The density plot of the scattered sound pressure signal (equivalent to figure 5 in the previous subsection) is presented in figure 6. It is obvious that the scattered sound signal has to be symmetric with respect to the direction of shock propagation. The

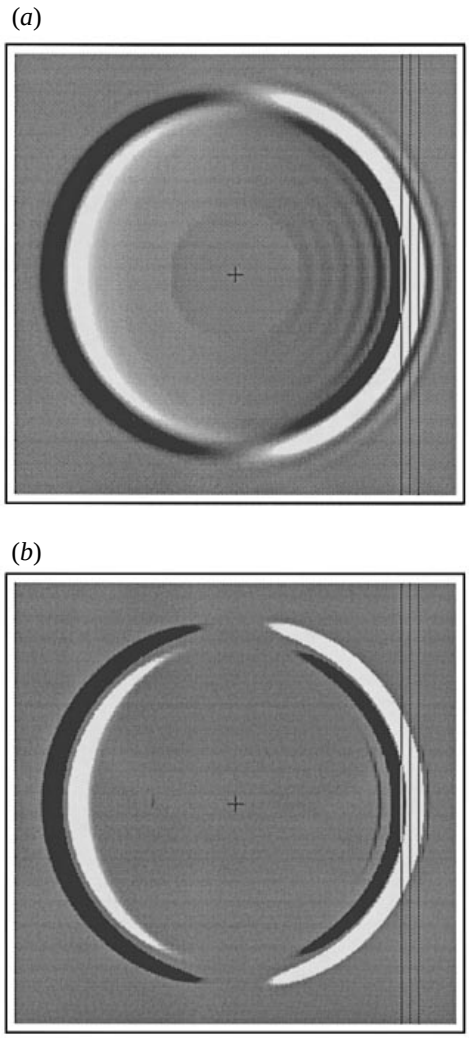

FIGURE 6. Density plot of the scattered sound pressure signal for the scattering by the model hot spot.

scattered sound signal essentially consists of two successive cylindrical, nearly dipolar sound waves. In the forward-scattering region the outer sound wave is a compression wave while the inner one is an expansion wave. In the backward-scattering region it is the other way round. The sound scattering has its minimum perpendicular to the direction of shock wave propagation.

Hamernik & Dosanjh (1973) carried out an experiment in order to investigate shock–hot-spot interactions where the hot spot was produced by a copper-wire explosion. When a shock passed over the hot spot, a cylindrical sound wave was generated, the amplitude of which was measured by Mach–Zehnder interferometry. The amplitude obtained in this way is nearly dipolar, but not really symmetric with respect to the direction of shock propagation. A radial cross-section of the scattered sound pressure at $\phi = \pi$ features only the outer minimum but not the inner maximum found in our calculations. It is believed that the differences between experiment and

theory are due to an insufficient experimental set-up since the presumed medium at rest could probably not be guaranteed in the experiment due to the wire explosion. Additionally, the shock strengths were not weak, which renders a quantitative comparison between experimental and theoretical results impossible.

5. Conclusions

A semi-analytical theory for the calculation of the scattering of a plane sound wave by a single cylindrical vortex was developed. As a special case, the scattering by a cylindrical inhomogeneity was considered. The theory made use of the acoustic approximation and assumed that the dependence of the base flow variables on time and on the azimuthal angle ϕ can be neglected during the scattering process.

It was shown that a formal analogy between three-dimensional quantum-mechanical and two-dimensional acoustic scattering theories exists which was mainly employed to estimate the computational effort as a function of the frequency ω of the incoming sound wave. Contrary to the quantum-mechanical scattering theory, there are singularities in the modified wave equation for finite but non-zero radii if the scattering by a vortex is considered. It was shown how these singularities can be treated. A consequence of the existence of these singularities is that the scattering by a vortex is inelastic whereas the scattering by a hot spot is elastic.

The sound-scattering theory was applied to the problem of shock–vortex interaction and shock–hot-spot interaction. The shock, actually a periodic sequence of weak plane shocks, is represented by a sequence of N-waves, which can by approximated by a Fourier sum of plane sinusoidal sound waves. In this way shock–vortex interaction was traced back to the problem of sound scattering by a vortex. The calculated cylindrical sound waves, which are formed when the shock is passing over the vortex/hot spot, are in qualitative agreement with experimental results for both cases. Quantitative comparisons could not be made since no experiments with really weak shocks were known.

Further investigations should be carried out in order to tackle the inverse scattering problem for a compressible cylindrical vortex. The formal analogy between quantum-mechanical and acoustic direct scattering theories may possibly serve as a basis for transferring results of the inverse scattering problem from quantum mechanics to acoustics. A satisfactory solution of the inverse scattering problem could be of practical relevance for determining the location and strength of vortices at airports (Ferziger 1974).

Appendix A

(r, ϕ, z)	dimensional cylindrical coordinate system
R	dimensional vortex radius
(x, ϕ)	non-dimensional polar coordinate system
x_s	non-dimensional radial location of a singularity
(ξ_1, ξ_2)	non-dimensional Cartesian coordinate system
$\rho_g(r, \phi, t), p_g(r, \phi, t),$ $u_g(r, \phi, t), v_g(r, \phi, t), w_g = 0$	dimensional sum of base flow and sound variables: density, pressure, radial, azimuthal and axial velocities.
$\bar{\rho}(r), \bar{p}(r), \bar{v}(r), \bar{\Gamma}(r),$ $\bar{s}(r), \bar{T}(r), \bar{c}(r)$	dimensional base flow variables: density, pressure, azimuthal velocity, circulation, entropy, temperature and sound velocity

	non-dimensional base flow variables:
$Q(x), P(x), V(x),$ $S(x), T(x), c(x)$	density, pressure, azimuthal velocity, entropy, temperature and sound velocity
$a_1(x), a_2(x), a_3(x),$ $b_1(x), f_1(x), g_1(x)$	functions defined through non-dimensional base flow variables (see (3.15), and below (3.21) and (B 1))
	dimensional sound perturbation variables:
$\dot{\rho}(r,\phi,t), \dot{p}(r,\phi,t),$ $\dot{u}(r,\phi,t), \dot{v}(r,\phi,t), \dot{w}=0$	density, pressure, radial, azimuthal and axial velocity components
	dimensional Fourier components of the sound variables:
$\hat{\rho}_{\bar{\omega}}(r,\phi), \hat{p}_{\bar{\omega}}(r,\phi),$ $\hat{u}_{\bar{\omega}}(r,\phi), \hat{v}_{\bar{\omega}}(r,\phi)$	density, pressure, radial and azimuthal velocities
$\hat{\rho}_{\bar{\omega}n}(r), \hat{p}_{\bar{\omega}n}(r)$	dimensional partial density and pressure waves
$\hat{u}_{\bar{\omega}n}(r), \hat{v}_{\bar{\omega}n}(r)$	dimensional partial radial and azimuthal velocity waves
$\rho_{\omega n}(x), p_{\omega n}(x)$	non-dimensional partial density and pressure waves
$u_{\omega n}(x), v_{\omega n}(x)$	non-dimensional radial and azimuthal velocity waves
$\bar{\omega}, \omega$	dimensional and non-dimensional frequency
$\boldsymbol{k}, k = \lvert\boldsymbol{k}\rvert$	non-dimensional wave vector and wavenumber ($\omega = k$ far outside the vortex/hot-spot)
n	azimuthal separation parameter in $\mathrm{e}^{\mathrm{i}n\phi}$
$\kappa = 1.4$	ratio of specific heats
$J_n(kx), Y_n(kx)$	Bessel functions of the first and second kind
δ_{rn}, δ_{in}	phase angles for nth partial wave;
(δ_n)	for elastic scattering $\delta_{rn} = \delta_{in} =: \delta_n$.
$f(\phi)$	scattering amplitude
$(\mathrm{d}\sigma_S/\mathrm{d}\phi)(\phi), \sigma_S$	differential and total cross-section
subscript '∞'	denotes base flow variable for large radii
superscript 'in'	denotes incoming plane sound wave
superscript 'sc'	denotes scattered sound wave
superscript 'el'	stands for 'elastic' and refers to scattering by a hot spot
superscript 'inel'	stands for 'inelastic' and refers to scattering by a vortex

Appendix B. Equations for non-homentropic base flow

The *basic equations* for a non-homentropic base flow are

$$\left.\begin{aligned} \mathrm{i}\left(Q\,a_1^2 + a_3\right)\,u_{\omega n} - Q\,a_1\,b_1\,v_{\omega n} &= -a_1\,\frac{\mathrm{d}p_{\omega n}}{\mathrm{d}x} + a_1\,g_1\,p_{\omega n}, \\ Q\,f_1\,u_{\omega n} + \mathrm{i}\,Q\,a_1\,v_{\omega n} &= -\mathrm{i}\,\frac{n}{x}\,p_{\omega n}, \\ \frac{\mathrm{d}u_{\omega n}}{\mathrm{d}x} + \frac{1}{x}\,u_{\omega n} + \frac{1}{c^2 Q}\frac{\mathrm{d}P}{\mathrm{d}x}\,u_{\omega n} + \mathrm{i}\,\frac{n}{x}\,v_{\omega n} &= -\mathrm{i}\,\frac{a_1}{c^2\,Q}\,p_{\omega n}, \end{aligned}\right\} \tag{B 1}$$

where a_3 stands for

$$a_3 := g_1\left(\frac{\mathrm{d}P}{\mathrm{d}x} - c^2\,\frac{\mathrm{d}Q}{\mathrm{d}x}\right).$$

The system of equations (3.18) has to be replaced by

$$\left.\begin{aligned} p'_{\omega n} &= \mathrm{i}\left(-Q\,a_1 - \frac{a_3}{a_1} + \frac{Q\,b_1\,f_1}{a_1}\right) u_{\omega n} + \left(g_1 - \frac{b_1\,n}{a_1\,x}\right) p_{\omega n}, \\ u'_{\omega n} &= \left(\frac{f_1\,n}{a_1\,x} - \frac{1}{x} - \frac{1}{c^2\,Q}\,\frac{\mathrm{d}P}{\mathrm{d}x}\right) u_{\omega n} + \mathrm{i}\left(\frac{n^2}{Q\,a_1\,x^2} - \frac{a_1}{c^2\,Q}\right) p_{\omega n}. \end{aligned}\right\} \tag{B 2}$$

The coefficient functions $co_1(x)$ and $co_0(x)$ in the modified wave equation (3.19) contain 18 and 32 terms instead of 6 and 9 in (3.20) and (3.21). The general expressions for both coefficient functions were calculated with the aid of MATHEMATICA (Wolfram 1992). We do not give them here for brevity.

Appendix C. Frictional effects

In this Appendix we investigate the influence small friction has on the partial sound pressure waves $p_{\omega n}(x)$. Despite the incorporation of friction, we will still assume that the base flow is approximately homentropic, in order to keep the length of the equations still manageable. The compressible Navier–Stokes equations are

$$\rho_g\left(\frac{\partial \boldsymbol{v}_g}{\partial t} + \left(\boldsymbol{v}_g\cdot\nabla\right)\,\boldsymbol{v}_g\right) = -\mathrm{grad}\,p_g + \bar{\mu}\Delta\boldsymbol{v}_g + \left(\bar{\mu}_P + \tfrac{1}{3}\bar{\mu}\right)\,\mathrm{grad}\,\mathrm{div}\,\boldsymbol{v}_g. \tag{C 1}$$

The two friction coefficients are denoted by $\bar{\mu}$ (= dynamic shear viscosity) and $\bar{\mu}_P$ (= dynamic bulk viscosity). Since we need these equations in cylindrical coordinates, they are rewritten as

$$\rho_g\left(\frac{\partial \boldsymbol{v}_g}{\partial t} + \left(\boldsymbol{v}_g\cdot\nabla\right)\,\boldsymbol{v}_g\right) = -\mathrm{grad}\,p_g + \alpha\,\mathrm{grad}\,\mathrm{div}\,\boldsymbol{v}_g - \beta\,\mathrm{rot}\,\mathrm{rot}\,\boldsymbol{v}_g \tag{C 2}$$

with $\beta := \bar{\mu}$, and $\alpha := \bar{\mu}_P + \frac{4}{3}\bar{\mu}$. In order to derive the *basic equations including friction* we proceed as in §3.1. Two Reynolds numbers Re_1 and Re_2 have to be defined:

$$Re_1 := \frac{\bar{\rho}_\infty\bar{c}_\infty R}{\alpha} \qquad \text{and} \qquad Re_2 := \frac{\bar{\rho}_\infty\bar{c}_\infty R}{\beta}. \tag{C 3}$$

We eventually arrive at

$$\left.\begin{aligned} \mathrm{i}\,Q\,a_1\,u_{\omega n} - Q\,b_1\,v_{\omega n} &= -\frac{\mathrm{d}p_{\omega n}}{\mathrm{d}x} + g_1\,p_{\omega n} + D_1, \\ Q\,f_1\,u_{\omega n} + \mathrm{i}\,Q\,a_1\,v_{\omega n} &= -\frac{\mathrm{i}\,n}{x}\,p_{\omega n} + D_2, \\ \frac{\mathrm{d}u_{\omega n}}{\mathrm{d}x} + \left(\frac{1}{x} + \frac{1}{Q}\,\frac{\mathrm{d}Q}{\mathrm{d}x}\right) u_{\omega n} + \mathrm{i}\,\frac{n}{x}\,v_{\omega n} &= -\mathrm{i}\,\frac{1}{c^2\,Q}\,a_1\,p_{\omega n}, \end{aligned}\right\} \tag{C 4}$$

which is precisely the same as (3.16) apart from the frictional terms D_1 and D_2.

Now we turn to the friction-including proof of the phase jump at $x = x_{s1}$ where $a_1(x_{s1}) = 0$. The two fundamental solutions of (3.19) formulated as series about $x = x_{s1}$ are of the following form:

$$p_{1\omega n}(x) = (x - x_{s1})\,\mathscr{P}_1(x),$$

$$p_{2\omega n}(x) = \beta_1\,(x - x_{s1})\,\mathscr{P}_1(x)\ln(x - x_{s1}) - \mathscr{P}_2(x),$$

where $\mathscr{P}_1(x)$ and $\mathscr{P}_2(x)$ are power series about $x = x_{s1}$ with the first term being equal to one. The first fundamental solution $p_{1\omega n}(x)$ is analytic in $x = x_{s1}$ whereas the first

derivative of the second solution has a logarithmic singularity there. Thus, the partial azimuthal sound velocity $v_{\omega n}(x)$ possesses the same singularity and consequently $v_\omega(x,\phi)$ too, which is physically impossible. We conclude therefore, that $p_{2\omega n}(x)$ has to be replaced by some other analytic function $p_{21}(x)$ in a small neighbourhood $\mathscr{U}$ around $x = x_{s1}$. Outside $\mathscr{U}$, $p_{21}(x)$ should become $p_{2\omega n}(x)$. The function $p_{21}(x)$ can be obtained if a friction-including equation is considered instead of (3.19). This equation must turn into (3.19) in the limit of negligible friction.

An approximate friction-including wave equation for $p_{\omega n}(x)$ can be found as follows. We proceed as we did in deriving the frictionless wave equation (3.19), but retain D_1 and D_2 in the two momentum equations. In a second step we eliminate $u_{\omega n}(x)$ and $v_{\omega n}(x)$ in D_1 and D_2 by means of

$$u_{\omega n} = -\mathrm{i}\frac{a_1}{Q\,a_2}\,\frac{\mathrm{d}p_{\omega n}}{\mathrm{d}x} + \mathrm{i}\,\frac{a_1\,g_1 - b_1\,n/x}{Q\,a_2}\,p_{\omega n} \tag{C 5}$$

and

$$v_{\omega n} = -\frac{f_1}{Q\,a_2}\,\frac{\mathrm{d}p_{\omega n}}{\mathrm{d}x} + \frac{a_1\,n/x - f_1\,g_1}{Q\,a_2}\,p_{\omega n}. \tag{C 6}$$

Equations (C 5) and (C 6) can be found by inserting (3.16*b*) into (3.16*a*). Neglected terms are of $O(1/(Re_2)^2)$. The resulting differential equation is of fourth order and has no singularity in $x = x_{s1}$, provided $a_2(x_{s1}) \neq 0$. This approximate friction-including wave equation assumes the form

$$\begin{aligned} rco_4(x)p^{\mathrm{iv}}_{\omega n}(x) + rco_3(x)p'''_{\omega n}(x) + (oco_2(x) + rco_2(x))\,p''_{\omega n}(x) \\ + (oco_1(x) + rco_1(x))\,p'_{\omega n}(x) + (oco_0(x) + rco_0(x))\,p_{\omega n}(x) = 0, \end{aligned} \tag{C 7}$$

where

$$\frac{oco_1(x)}{oco_2(x)} = co_1(x) \qquad \text{and} \qquad \frac{oco_0(x)}{oco_2(x)} = co_0(x).$$

All coefficient functions with first letter r are of $O(1/Re_2)$. We neglect $rco_2(x), rco_1(x)$ and $rco_0(x)$ from now on. All remaining coefficient functions are developed into power series about the singularity $x = x_{s1}$. We obtain for $oco_1(x)$

$$oco_1(x) = \left[\frac{-1}{Q(x)a_2(x)}\left(-\frac{n}{x}\,b_1(x) + \frac{n}{x}\,f_1(x) - a'_1(x)\right)\right]_{x=x_{s1}} + O(x - x_{s1}). \tag{C 8}$$

The first term on the right-hand side vanishes since $a'_1(x) = (n/x)\,(f_1(x) - b_1(x))$ and $a_2(x_{s1}) \neq 0$ as presumed. Thus, we have

$$oco_1(x) = \sum_{j=1}^{\infty} \alpha_{(1)j}(x - x_{s1})^j$$

as well as

$$\left.\begin{aligned} rco_4(x) &= \frac{\mathrm{i}}{Re_2}\sum_{j=0}^{\infty}\alpha_{(4)j}(x - x_{s1})^j, \qquad rco_3(x) = \frac{\mathrm{i}}{Re_2}\sum_{j=0}^{\infty}\alpha_{(3)j}(x - x_{s1})^j, \\ oco_2(x) &= \sum_{j=1}^{\infty}\alpha_{(2)j}(x - x_{s1})^j, \qquad oco_0(x) = \sum_{j=0}^{\infty}\alpha_{(0)j}(x - x_{s1})^j. \end{aligned}\right\} \tag{C 9}$$

We introduce a new variable η which replaces $x - x_{s1}$:

$$\epsilon \cdot \eta = (x - x_{s1}) \quad \text{with} \quad \tilde{p}(\eta) := p_{\omega n}(x) \quad \text{and} \quad \epsilon \ll 1. \tag{C 10}$$

We insert the series expansions (C 9) into equation (C 7), divide by $\alpha_{(2)1}$ and rearrange the terms in the order of powers of ϵ, thereby obtaining

$$\frac{1}{Re_2}\frac{1}{\epsilon^3}\frac{\alpha_{(4)0}}{\alpha_{(2)1}}\,\mathrm{i}\,\frac{\mathrm{d}^4}{\mathrm{d}\eta^4}\,\tilde{p}(\eta)+\eta\,\frac{\mathrm{d}^2}{\mathrm{d}\eta^2}\,\tilde{p}(\eta)+\frac{1}{Re_2}\frac{1}{\epsilon^2}\,\mathrm{i}\left(\frac{\alpha_{(4)1}}{\alpha_{(2)1}}\,\eta\,\frac{\mathrm{d}^4}{\mathrm{d}\eta^4}\,\tilde{p}(\eta)+\frac{\alpha_{(3)0}}{\alpha_{(2)1}}\,\frac{\mathrm{d}^3}{\mathrm{d}\eta^3}\,\tilde{p}(\eta)\right)$$
$$=-\epsilon\left(\frac{\alpha_{(2)2}}{\alpha_{(2)1}}\,\eta^2\,\frac{\mathrm{d}^2}{\mathrm{d}\eta^2}\,\tilde{p}(\eta)+\frac{\alpha_{(1)1}}{\alpha_{(2)1}}\,\eta\,\frac{\mathrm{d}}{\mathrm{d}\eta}\,\tilde{p}(\eta)+\frac{\alpha_{(0)0}}{\alpha_{(2)1}}\,\tilde{p}(\eta)\right)+O(\epsilon^2). \tag{C 11}$$

The first two terms on the left-hand side of (C 11) should be of $O(1)$, and all other terms of (C 11) of $O(\epsilon)$. This is achieved by setting

$$\frac{1}{Re_2}\frac{1}{\epsilon^3}\frac{\alpha_{(4)0}}{\alpha_{(2)1}}=1. \tag{C 12}$$

Since $p_{21}(x)$ should be bounded for $x=x_{s1}$, the assumption

$$p_{21}(x)=1+\epsilon p_{21\epsilon}(x) \tag{C 13}$$

is made for $x\in\mathscr{U}$. Inserting $\tilde{p}_{21}(\eta)=p_{21}(x)$ into equation (C 11), neglecting all terms $\sim O(\epsilon^2)$ and dividing by ϵ yields a differential equation for $\tilde{p}_{21\epsilon}(\eta)$:

$$\mathrm{i}\,\frac{\mathrm{d}^4}{\mathrm{d}\eta^4}\,\tilde{p}_{21\epsilon}(\eta)+\eta\,\frac{\mathrm{d}^2}{\mathrm{d}\eta^2}\,\tilde{p}_{21\epsilon}(\eta)=-\frac{\alpha_{(0)0}}{\alpha_{(2)1}}. \tag{C 14}$$

The solutions $p''_{21\epsilon}(\eta)$ of (C 14) are Airy functions (see Abramowitz & Stegun 1964)

$$\eta^{1/2}\,H^{(1)}_{1/3}\left(\tfrac{2}{3}\,(\mathrm{i}\,\eta)^{3/2}\right)\quad\text{and}\quad\eta^{1/2}\,H^{(2)}_{1/3}\left(\tfrac{2}{3}\,(\mathrm{i}\,\eta)^{3/2}\right), \tag{C 15}$$

where $H^{(1)}$ and $H^{(2)}$ are Hankel functions of the first and second kind. By means of the Airy functions given in (C 15) one can construct $\tilde{p}_{21\epsilon}(\eta)$ and, thus, $p_{21}(x)$. This is done in a way similar to the treatment of the singularity in the Orr–Sommerfeld problem (cf. Tollmien 1929). The Hankel functions have an analytic asymptotic representation valid in the whole lower η-half-plane, but not in the whole upper η-half-plane. Therefore, one has to choose an integration path in the lower η-half-plane. With the aid of MATHEMATICA we obtained

$$rco_4(x)=\frac{\mathrm{i}}{Re_1}\,\frac{a_1^2(x)}{[a_2(x)Q(x)]^2}+\frac{\mathrm{i}}{Re_2}\,\frac{b_1(x)f_1(x)}{[a_2(x)Q(x)]^2}\;\Rightarrow\;\alpha_{(4)0}=\frac{1}{Q^2(x_{s1})}\,\frac{1}{b_1(x_{s1})f_1(x_{s1})}$$

and

$$oco_2(x)=\frac{a_1(x)}{a_2(x)Q(x)}\;\Rightarrow\;\alpha_{(2)1}=\frac{\mathrm{d}}{\mathrm{d}x}\,(oco_2(x))\bigg|_{x=x_{s1}}=\frac{a_1'(x_{s1})}{b_1(x_{s1})f_1(x_{s1})Q(x_{s1})}.$$

Consequently,

$$\frac{\alpha_{(4)0}}{\alpha_{(2)1}}=\frac{Q(x)}{a_1'(x)}\bigg|_{x=x_{s1}}=\frac{Q(x_{s1})}{nW'(x_{s1})}, \tag{C 16}$$

provided that $W'(x_{s1})\neq 0$. Let ϵ be real. According to (C 12) and since $n>0$, $Q(x_{s1})>0$, and $Re_2>0$, one concludes

$$\epsilon\;\begin{matrix}>\\<\end{matrix}\;0\quad\longleftrightarrow\quad\frac{\alpha_{(4)0}}{\alpha_{(2)1}}\;\begin{matrix}>\\<\end{matrix}\;0\quad\longleftrightarrow\quad W'(x_{s1})\;\begin{matrix}>\\<\end{matrix}\;0. \tag{C 17}$$

This means: for $W'(x_{s1})<0$ we have to integrate in the upper x-half-plane. This corresponds to a phase jump of $-\pi$ of the second frictionless fundamental solution $p_{2\omega n}(x)$ at $x=x_{s1}$ when the increasing independent variable x passes over x_{s1}. For

$W'(x_{s1}) > 0$, we would get a phase jump of $+\pi$. This is precisely the same result as the one furnished by the causality argument.

REFERENCES

Abramowitz, M. & Stegun, I. A. 1964 *Handbook of Mathematical Functions*. National Bureau of Standards.

Booker, J. R. & Bretherton, F. P. 1967 The critical layer for internal gravity waves in a shear flow. *J. Fluid Mech.* **27**, 513–539.

Broadbent, E. G. 1977 Acoustic ray theory applied to vortex refraction. *J. Inst. Maths Applics.* **19**, 1–27.

Colonius, T., Lele, S. K. & Moin, P. 1994 The scattering of sound waves by a compressible vortex – numerical simulations and analytical solutions. *J. Fluid Mech.* **260**, 271–298.

Dosanjh, D. S. & Weeks, T. M. 1965 Interaction of a starting vortex as well as a vortex street with a traveling shock wave. *AIAA J.* **3**, 216–223.

Ellzey, J. L., Picone, M. & Oran, E. S. 1992 The interaction of a shock with a compressible vortex. *NRL Mem. Rep.* 6919. Naval Research Lab., Washington.

Ferziger, J. H. 1974 Low frequency acoustic scattering from a trailing vortex. *J. Acoust. Soc. Am.* **56**, 1705–1707.

Fetter, A. L. 1964 Scattering of sound by a classical vortex. *Phys. Rev.* **136**, 1488–1493.

Hamernik, R. P. & Dosanjh, D. S. 1973 Generation of acoustic waves during the passage of a shock wave through a heated gaseous element. *J. Acoust. Soc. Am.* **53**, 921–925.

Hollingsworth, M. A. & Richards, E. J. 1955 A schlieren study of the interaction of a vortex and a shock wave. *Aeron. Res. Counc. Rep.* 17985. Fluid Motion Subcommittee 2323, London.

Howe, M. S. 1983 On the scattering of sound by a vortex ring. *J. Sound Vib.* **87**, 567–571.

Kambe, T. 1982 Scattering of sound by vortex systems. *J. Japan Soc. Fluid Mech.* **1**, 149–165.

Kambe, T. & Mya Oo, U. 1981 Scattering of sound by a vortex ring. *J. Phys. Soc. Japan* **50**, 3507–3516.

Kirde, K. 1962 Untersuchungen über die zeitliche Weiterentwicklung eines Wirbels mit vorgegebener Anfangsverteilung. *Ingenieur–Archiv* **37**, 385–404.

Klimow, V. V. 1988 Influence of a vortex velocity field on the propagation of sound waves. *Sov. Phys. Acoust.* **34**, 154–157.

Lee, S. & Bershader, D. 1994 Head-on parallel blade–vortex interaction. *AIAA J.* **32**, 16–22.

Lin, C. C. 1955 *The Theory of Hydrodynamic Stability*. Cambridge University Press.

Mandella, M. & Bershader, D. 1987 Quantitative study of the compressible vortex: generation, structure and interaction with airfoils. *AIAA Paper* 87-0328.

McKenzie, J. F. 1979 Critical level behavior of ion-cyclotron-waves. *J. Plasma Phys.* **22**, 361–376.

Moore, D. W. & Saffman, P. G. 1973 Axial flow in laminar trailing vortices. *Proc. R. Soc. Lond.* A **333**, 491–508.

Morse, P. M. & Feshbach, H. 1953 *Methods of Theoretical Physics,* Vol. I, p. 620. McGraw–Hill.

Müller, E.-A. & Matschat, K. R. 1959 The scattering of sound by a single vortex and by turbulence. *Tech. Rep.* MPI für Strömungsforschung Göttingen.

Obermeier, F. 1968 Die Wechselwirkung zwischen Strömungsfeldern und Schallfeldern als singuläres Störungsproblem. PhD Thesis, MPI für Strömungsforschung Göttingen.

O'Shea, S. 1975 Sound scattering by a potential vortex. *J. Sound Vib.* **43**, 109–116.

Ram, G. S. & Ribner, H. S. 1959 The sound generated by interaction of a single vortex with a shock wave. *UTIA Rep.* 61. University of Toronto.

Rayleigh, Lord 1945 *The Theory of Sound,* Vol. II, pp. 149–152, Second edn. Dover.

Reinschke, J. 1994 Schallstreuung am zylindrischen Einzelwirbel sowie Stoß–Wirbel–Wechselwirkung und Stoß–hot-spot–Wechselwirkung. *Bericht* 21/1994. MPI für Strömungsforschung Göttingen.

Ribner, H. S. 1954 Convection of a pattern of vorticity through a shock wave. *NACA Rep.* 1165.

Ribner, H. S. 1955 Shock–turbulence interaction and the generation of noise. *NACA Rep.* 1233.

Ribner, H. S. 1985 Cylindrical sound wave generated by shock–vortex interaction. *AIAA J.* **23**, 1708–1715.

SCHÜRMANN, O. 1994 Wechselwirkung einer kompressiblen Wirbelstraße mit einem Tragflügelprofil. PhD Thesis, MPI für Strömungsforschung Göttingen.

TAYLOR, J. R. 1972 *Scattering Theory*. John Wiley & Sons.

TOLLMIEN, W. 1929 Über die Entstehung der Turbulenz, 1. Mitteilung. *Nachr. Ges. Wiss. Göttingen, Math. Phys. Klasse* **21**, 21–44.

TOLLMIEN, W. 1935 Ein allgemeines Kriterium der Instabilität laminarer Geschwindigkeitsverteilungen. *Nachr. Ges. Wiss. Göttingen, Math. Phys. Klasse, Fachgruppe I* **1**, 79–114.

TOLLMIEN, W. 1947 Asymptotische Integration der Störungsdifferentialgleichung ebener laminarer Strömungen bei hohen Reynoldsschen Zahlen. *Z. Angew. Math. Mech.* **25/27**, 33–83.

TUNG, C., PUCCI, S. L., CARADONNA, F. X. & MORSE, H. A. 1983 The structure of trailing vortices generated by model rotor blades. *Vertica* **7**, 33–43.

WOLFRAM, S. 1992 *Mathematica. Ein System für Mathematik auf dem Computer,* Second edn. Addison–Wesley.